Int. J. Solids Structures, 1973, Vol. 9, pp. 177 to 192. Pergamon Press. Printed in Great Britain

IMPERFECTION-SENSITIVITY OF A WIDE INTEGRALLY STIFFENED PANEL UNDER COMPRESSION

VIGGO TVERGAARD

Department of Solid Mechanics,
The Technical University of Denmark, Lyngby, Denmark

Abstract—The initial post-buckling behaviour is determined for an integrally stiffened wide panel under compression. Overall buckling of the panel as a wide Euler column and local buckling of the plates between the stiffeners are considered.

Designing the panel so that the critical bifurcation load is the highest possible for a given amount of material per unit width tends to lead to a structure in which Euler-type buckling and local buckling occur simultaneously. It is shown that such a panel is very sensitive to geometrical imperfections. Thus, the critical bifurcation load cannot be reached in a practical structure and the two-mode design may not be optimal.

INTRODUCTION

IN COMPRESSION members containing thin plates, both local buckling of the plate elements and Euler-type buckling of the whole structure can occur. It has occasionally been suggested that optimum design of such structures is obtained when general buckling and local buckling occur simultaneously. However, as stated by Koiter [1], this is questionable, since interaction between the two independent buckling modes may result in an imperfection-sensitive structure.

An investigation of the interaction between local buckling and column failure has been made by van der Neut [2]. He considered a simplified model of a column consisting of two load carrying flanges connected by webs, which are rigid in shear and laterally but which have no longitudinal stiffness. Thus in this model, the two load-carrying flanges behave exactly like a simply supported plate in compression. This model proved to be strongly imperfection-sensitive in the vicinity of the "optimal" design. Very recently Koiter and Kuiken [3] have treated the same problem by application of the general nonlinear theory of elastic stability, and Thompson and Lewis [4] have calculated optimal designs of idealized columns with imperfect flanges.

In the present paper, the initial post-buckling behaviour of a wide, integrally stiffened panel subject to compression is determined. Here, there are the possibilities of buckling of the whole panel as a wide Euler column and of local buckling of the plate between the stiffeners. Special attention is directed to cases in which the two buckling modes occur simultaneously, with a view to further establishing the imperfection-sensitivity that may be inherent in such "optimal" designs.

1. NONLINEAR EQUILIBRIUM EQUATIONS

We consider (Fig. 1) a panel that is infinitely wide in the y-direction, with a constant spacing b between the stiffeners and the distance a between the simply supported edges.

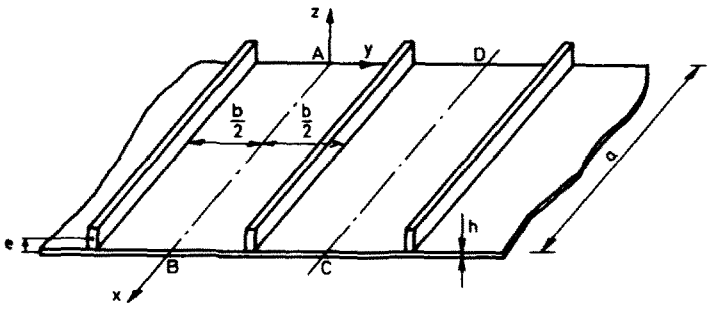

FIG. 1. Part of plane, integrally stiffened panel.

The plate thickness is h and the eccentricity e of the stiffeners is taken as positive in the z-direction.

We take into account the torsional stiffness of the stringers but neglect their tangential bending stiffness. For a cylindrical panel under axial compression, Koiter [5] neglected both these contributions and discussed the approximations made. For the same structure, the influence of torsional stiffness has recently been calculated by Stephens [6].

The membrane strains of the plate are taken to be

$$\begin{aligned} \varepsilon_x &= u_{,x} + \tfrac{1}{2}w_{,x}^2 \\ \varepsilon_y &= v_{,y} + \tfrac{1}{2}w_{,y}^2 \\ \varepsilon_{xy} &= \tfrac{1}{2}(u_{,y} + v_{,x}) + \tfrac{1}{2}w_{,x}w_{,y} \end{aligned} \tag{1.1}$$

where u, v and w are the displacements of the middle surface in the x, y and z directions, respectively, and the bending strains are given by

$$\kappa_x = w_{,xx}, \qquad \kappa_y = w_{,yy}, \qquad \kappa_{xy} = w_{,xy}. \tag{1.2}$$

The bending strain in a stiffener is taken to be the same as in the plate, $w_{,xx}$, and the axial strain of the neutral axis is taken to be

$$\varepsilon_s = \varepsilon_x - ew_{,xx} + \tfrac{1}{2}e^2 w_{,xy}^2. \tag{1.3}$$

The last term on the right-hand side of (1.3) is due to the rotation of the stiffener around its line of attachment to the plate. Here, we have neglected all nonlinear effects of the tangential displacements of the plate middle surface, as is traditionally done in the expressions (1.1).

The usual stress–strain relationships are assumed for the plate

$$\begin{aligned} N_x &= \frac{Eh}{1-\nu^2}(\varepsilon_x + \nu\varepsilon_y), & M_x &= D(\kappa_x + \nu\kappa_y) \\ N_{xy} &= \frac{Eh}{1+\nu}\varepsilon_{xy}, & M_{xy} &= D(1-\nu)\kappa_{xy} \\ N_y &= \frac{Eh}{1-\nu^2}(\varepsilon_y + \nu\varepsilon_x), & M_y &= D(\kappa_y + \nu\kappa_x) \end{aligned} \tag{1.4}$$

and for a stiffener

$$N_s = E_s A_s \varepsilon_s, \qquad M_s = E_s I_s w_{,xx}, \qquad M_{Vs} = G_s K_s w_{,xy}. \tag{1.5}$$

Here E, D and G denote Young's modulus, the plate bending stiffness and the shear modulus, respectively, and subscript s refers to a stiffener.

Using the calculus of variations, the internal virtual work in one plate section can be written as

$$\begin{aligned}
&\int_0^a \int_{-b/2}^{b/2} (N_x \delta\varepsilon_x + 2N_{xy}\delta\varepsilon_{xy} + N_y \delta\varepsilon_y + M_x \delta\kappa_x + 2M_{xy}\delta\kappa_{xy} + M_y \delta\kappa_y)\,\mathrm{d}y\,\mathrm{d}x \\
&\quad = \int_0^a \int_{-b/2}^{b/2} [-N_{x,x} - N_{xy,y})\delta u + (-N_{yx,x} - N_{y,y})\delta v + (M_{x,xx} \\
&\qquad + 2M_{xy,xy} + M_{y,yy} - N_x w_{,xx} - 2N_{xy} w_{,xy} - N_y w_{,yy} \\
&\qquad - (N_{x,x} + N_{xy,y}) w_{,x} - (N_{yx,x} + N_{y,y}) w_{,y})\delta w]\,\mathrm{d}y\,\mathrm{d}x \\
&\qquad + \int_0^a [N_{xy}\delta u + N_y \delta v + (-M_{y,y} - 2M_{xy,x} + N_{xy} w_{,x} + N_y w_{,y})\delta w + M_y \delta w_{,y}]_{y=-b/2}^{y=b/2}\,\mathrm{d}x \\
&\qquad + \int_{-b/2}^{b/2} [N_x \delta u + N_{xy}\delta v + (-M_{x,x} - 2M_{xy,y} + N_x w_{,x} + N_{xy} w_{,y})\delta w \\
&\qquad + M_x \delta w_{,x}]_{x=0}^{x=a}\,\mathrm{d}y + [[2M_{xy}\delta w]_{y=-b/2}^{y=b/2}]_{x=0}^{x=a}.
\end{aligned} \tag{1.6}$$

The internal virtual work in a stiffener is

$$\begin{aligned}
&\int_0^a (N_s \delta\varepsilon_s + M_s \delta w_{,xx} + M_{Vs}\delta w_{,yx})\,\mathrm{d}x \\
&\quad = \int_0^a [-N_{s,x}\delta u + (M_{s,xx} - eN_{s,xx} - N_{s,x} w_{,x} - N_s w_{,xx})\delta w \\
&\qquad + (-M_{Vs,x} - e^2 N_{s,x} w_{,xy} - e^2 N_s w_{,xxy})\delta w_{,y})\delta w_{,y}]\,\mathrm{d}x \\
&\qquad + [N_s \delta u + (-M_{s,x} + eN_{s,x} + N_s w_{,x})\delta w \\
&\qquad + (M_{Vs} + e^2 N_s w_{,xy})\delta w_{,y} + (M_s - eN_s)\delta w_{,x}]_{x=0}^{x=a}.
\end{aligned} \tag{1.7}$$

The internal virtual work in the whole structure is supposed to be equal to the external virtual work of prescribed surface and edge loads for all δu, δv and δw that do not violate boundary conditions. Thus, as loads are only applied on the edges, the equations of equilibrium for the plate are found by equating the coefficients of δu, δv and δw to zero in the surface integral of equation (1.6). The four conditions of equilibrium at a stringer are obtained by equating the coefficients of δu, δv, δw and $\delta w_{,y}$ to zero in the line integral along the stiffener, composed of contributions from the two plate sections meeting here and from the stiffener. We must further require continuity of the functions u, v, w and $w_{,y}$ at the stiffener.

Expressing the resultant membrane stresses by means of an Airy stress function

$$N_x = F_{,yy}, \qquad N_{xy} = -F_{,xy}, \qquad N_y = F_{,xx} \tag{1.8}$$

the equations of equilibrium in the middle plane are satisfied identically. Then the normal displacement $w(x, y)$ and the stress function $F(x, y)$ must satisfy one equilibrium equation and one compatibility equation

$$D\,\Delta\Delta w = F_{,yy}w_{,xx} - 2F_{,xy}w_{,xy} + F_{,xx}w_{,yy} \tag{1.9}$$

$$\frac{1}{Eh}\Delta\Delta F = w_{,xy}^2 - w_{,xx}w_{,yy} \tag{1.10}$$

where Δ is the Laplacian operator. Written in terms of w and F, the eight discontinuity conditions at a stiffener are ($+$ denoting the side of the stiffener in the positive y-direction and $-$ denoting the other side):

$$F_{,xx}^{+} - F_{,xx}^{-} = 0 \tag{1.11}$$

$$-F_{,xy}^{+} + F_{,xy}^{-} + N_{s,x} = 0 \tag{1.12}$$

$$-D(w_{,yyy}^{+} - w_{,yyy}^{-}) + eN_{s,xx} - E_sI_sw_{,xxxx}^{-} + N_sw_{,xx}^{-} = 0 \tag{1.13}$$

$$D(w_{,yy}^{+} - w_{,yy}^{-}) + G_sK_sw_{,yxx}^{-} + e^2N_sw_{,xxy}^{-} + e^2N_{s,x}w_{,xy}^{-} = 0 \tag{1.14}$$

$$F_{,yy}^{+} - F_{,yy}^{-} = 0 \tag{1.15}$$

$$(2+\nu)F_{,xxy}^{+} + F_{,yyy}^{+} - (2+\nu)F_{,xxy}^{-} - F_{,yyy}^{-} = 0 \tag{1.16}$$

$$w^{+} - w^{-} = 0 \tag{1.17}$$

$$w_{,y}^{+} - w_{,y}^{-} = 0 \tag{1.18}$$

where

$$N_s = E_sA_s\left[\frac{1}{Eh}(F_{,yy}^{-} - \nu F_{,xx}^{-}) - ew_{,xx}^{-} + \tfrac{1}{2}e^2w_{,xy}^{-2}\right]. \tag{1.19}$$

In the infinitely wide panel, the solution must be periodic in the y-direction. For the tangential displacement v this is enforced by the additional condition

$$\int_0^p \left[\frac{1}{Eh}(F_{,xx} - \nu F_{,yy}) - \tfrac{1}{2}w_{,y}^2\right] dy = \text{const.} \tag{1.20}$$

where integration is made over one whole period.

Boundary conditions at the simply supported edges can be taken to be

$$w = w_{,xx} = F = F_{,xx} = 0. \tag{1.21}$$

2. CLASSICAL BUCKLING

An infinitely wide plate without stiffeners has the buckling mode $w(x, y) = \sin(\pi x/a)$. When stiffeners are attached to the plate, the mode still resembles this Euler buckling mode as long as the stiffeners are relatively weak, and it is periodic with one period equal to the spacing between the stiffeners. However, when the stringers are sufficiently stiff, the plate buckles locally between the stiffeners before overall Euler-type buckling takes place. In this case, one period is equal to twice the spacing between the stiffeners.

Prior to buckling, the stress state is taken proportional to a stress state consisting of a constant resultant axial membrane stress N_x^0 in the plate and a constant force N_s^0 in the stiffeners. The other membrane stresses, the moments and the transverse deflections are identically zero.

Now we write the normal displacement and the stress function as $w = w_c$ and $F = \lambda_c F_0 + F_c$, where the term added to F_c accounts for the prebuckling solution for the perfect structure. The classical buckling equations are obtained by substituting these expressions in equations (1.9)–(1.18) and then linearizing the resulting equations with respect to w_c and F_c. The linear buckling equations are

$$D\,\Delta\Delta w_c - \lambda_c N_x^0 w_{c,xx} = 0 \tag{2.1}$$

$$\frac{1}{Eh}\Delta\Delta F_c = 0 \tag{2.2}$$

and the corresponding discontinuity conditions at the stiffeners have the form

$$F_{c,xx}^+ - F_{c,xx}^- = 0 \tag{2.3}$$

$$-F_{c,xy}^+ + F_{c,xy}^- + E_s A_s\left(\frac{1}{Eh}(F_{c,yyx}^- - \nu F_{c,xxx}^-) - e w_{c,xxx}^-\right) = 0 \tag{2.4}$$

$$-D(w_{c,yyy}^+ - w_{c,yyy}^-) + e(F_{c,xxy}^+ - F_{c,xxy}^-) - E_s I_s w_{c,xxxx}^- + \lambda_c N_s^0 w_{c,xx}^- = 0 \tag{2.5}$$

$$D(w_{c,yy}^+ - w_{c,yy}^-) + G_s K_s w_{c,yxx}^- + \lambda_c N_s^0 e^2 w_{c,xxy}^- = 0 \tag{2.6}$$

$$F_{c,yy}^+ - F_{c,yy}^- = 0 \tag{2.7}$$

$$(2+\nu)F_{c,xxy}^+ + F_{c,yyy}^+ - (2+\nu)F_{c,xxy}^- - F_{c,yyy}^- = 0 \tag{2.8}$$

$$w_c^+ - w_c^- = 0 \tag{2.9}$$

$$w_{c,y}^+ - w_{c,y}^- = 0. \tag{2.10}$$

Having the simple support boundary conditions (1.21) at the edges $x = 0, a$, we look for solutions in the form

$$w_c(x, y) = W(y)\sin\frac{k\pi x}{a} \tag{2.11}$$

$$F_c(x, y) = f(y)\sin\frac{k\pi x}{a} \tag{2.12}$$

where k is a positive integer. In the infinitely long periodic structure, the critical deflection function w_c and the stress function F_c for every plate section between two stiffeners are symmetric in y with respect to the centre of the section (Fig. 1). Using this, we find that the solutions (2.11) and (2.12) take the form

$$w_c = (c_1\cosh(r_1 y) + c_2\cos(r_2 y))\sin\frac{k\pi x}{a} \tag{2.13}$$

$$F_c = \left(c_3\cosh\frac{k\pi y}{a} + c_4 y\sinh\frac{k\pi y}{a}\right)\sin\frac{k\pi x}{a} \tag{2.14}$$

where

$$r_1 = \sqrt{\left\{\frac{k\pi}{a}\left[\frac{k\pi}{a}+\sqrt{(-\lambda_c N_x^0/D)}\right]\right\}}, \qquad r_2 = \sqrt{\left\{-\frac{k\pi}{a}\left[\frac{k\pi}{a}-\sqrt{(-\lambda_c N_x^0/D)}\right]\right\}}. \quad (2.15)$$

In the local coordinate system of the next plate section, taken in the positive y-direction, the same expressions apply, but here, instead of c_1, c_2, c_3 and c_4, we denote the constants c_5, c_6, c_7 and c_8. Substituting these expressions for w_c and F_c in the discontinuity conditions (2.3)–(2.10), we obtain eight linear, homogeneous equations for the constants $c_1, c_2, \ldots, c_8$ (Appendix). The critical buckling load λ_c is the smallest value of the parameter λ, for any integer value of k for which the determinant of the coefficient matrix vanishes.

Euler-type buckling occurs at $k = 1$, with identical modes for all plate sections between two stiffeners. Thus, the constants c_1, c_2, c_3 and c_4 are identical to c_5, c_6, c_7 and c_8, respectively, for this mode.

The smallest local buckling load usually occurs for an integer value of k close to the value of a/b. In the corresponding mode, the stress function F_c disappears identically, and the constants c_1 and c_2 are identical to $-c_5$ and $-c_6$, respectively.

3. INITIAL POST-BUCKLING THEORY

The general theory of initial post-buckling behaviour of elastic structures has been developed by Koiter [7, 8]. It is essentially a perturbation technique, which relies on the principle of stationary potential energy. For the special case of linear pre-buckling behaviour, Koiter's theory has been presented in a very convenient manner for applications, by Budiansky and Hutchinson [9–12]. In the present section, we shall just recall some of the main results of the theory, using mostly the notation of Ref. [9].

Generalized loads, stresses, strains and displacements will be denoted q, σ, ε and u, respectively. The internal virtual work of a stress field σ through a strain field $\delta\varepsilon$ for a structure is conveniently abbreviated in the form $\{\sigma, \delta\varepsilon\}$. The stress–strain relation and the strain–displacement relation are written

$$\sigma = H_1(\varepsilon) \quad (3.1)$$

$$\varepsilon = L_1(u) + \tfrac{1}{2}L_2(u) \quad (3.2)$$

where H_1 and L_1 are linear, homogeneous operators and L_2 is a quadratic, homogeneous operator. A bilinear, homogeneous operator L_{11} is defined by the identity

$$L_2(u+v) = L_2(u) + 2L_{11}(u, v) + L_2(v). \quad (3.3)$$

When λu_0 is the pre-buckling displacement, and n linearly independent buckling modes $u_c^{(1)}$, $u_c^{(2)}, \ldots$ are associated with the critical value λ_c of the load parameter, the complete displacement of the structure can be written as

$$u = \lambda u_0 + \sum_{i=1}^{n} \xi_i u_c^{(i)} + \tilde{u} \quad (3.4)$$

where the parameters ξ_i determine the amounts introduced of the corresponding buckling modes. The buckling modes are taken orthogonal to one another in the sense

$$\{\sigma_0, L_{11}(u_c^{(i)}, u_c^{(j)})\} = 0, \quad \text{for } i \neq j \quad (3.5)$$

where $\sigma_0 = H_1(L_1(u_0))$, and the additional displacement $\tilde{u}$ is orthogonal to each of the buckling modes.

If only a single mode is associated with λ_c, and the additional displacement is written as $\tilde{u} = \xi^2 u_2 + O(\xi^3)$, the following equilibrium equation relates the buckling mode amplitude ξ to the load parameter λ

$$(1-\lambda/\lambda_c)\xi + a\xi^2 + b\xi^3 + \ldots = \frac{\lambda}{\lambda_c}\bar{\xi} \tag{3.6}$$

where the right-hand side gives the lowest order influence of the geometrical imperfection $\bar{u} = \bar{\xi} u_c$ of the unloaded structure. The constants are given by the expressions

$$a = \frac{\frac{3}{2}\{\sigma_c, L_2(u_c)\}}{-\lambda_c\{\sigma_0, L_2(u_c)\}} \tag{3.7}$$

$$b = \frac{2\{\sigma_c, L_{11}(u_c, u_2)\} + \{\sigma_2, L_2(u_c)\}}{-\lambda_c\{\sigma_0, L_2(u_c)\}} \tag{3.8}$$

where $\sigma_c = H_1(L_1(u_c))$ and $\sigma_2 = H_1(L_1(u_2) + \frac{1}{2}L_2(u_c))$. The structure is imperfection-sensitive if either $a \neq 0$ or $a = 0, b < 0$. Formulae for the maximum value λ^* that the load parameter can reach in these cases are given in the references mentioned above. In the case $a = 0$, the relation between post-buckling and pre-buckling stiffness of the perfect structure is

$$K = \left[1 - \frac{\{\sigma_0, L_2(u_c)\}}{2\lambda_c b\{\sigma_0, L_1(u_0)\}}\right]^{-1}. \tag{3.9}$$

If there is more than one mode associated with λ_c, the equilibrium equations relating λ to the n buckling mode amplitudes ξ_i are

$$\xi_j(1-\lambda/\lambda_c) + \left[\left\{\sum_{i=1}^{n} \xi_i \sigma_c^{(i)}, L_{11}\left(\sum_{i=1}^{n} \xi_i u_c^{(i)}, u_c^{(j)}\right)\right\} + \frac{1}{2}\left\{\sigma_c^{(j)}, L_2\left(\sum_{i=1}^{n} \xi_i u_c^{(i)}\right)\right\}\right] \Big/ (-\lambda_c\{\sigma_0, L_2(u_c^{(j)})\}) + \ldots = \frac{\lambda}{\lambda_c}\bar{\xi}_j \quad \text{for } j = 1, 2, \ldots, n. \tag{3.10}$$

The generalized load–deflection relation for a perfect multimode structure is

$$\frac{\Delta}{\lambda_c \Delta_0} = \frac{\lambda}{\lambda_c} - \frac{1}{2}\sum_{i=1}^{n} \xi_i^2 \frac{\{\lambda_c \sigma_0, L_2(u_c^{(i)})\}}{\{\lambda_c \sigma_0, L_1(\lambda_c u_0)\}} \tag{3.11}$$

where the generalized displacement $\Delta = \{\sigma_0, L_1(u)\}$ has the property that $\lambda\Delta$ is the drop in potential energy of the external load.

4. TWO SIMULTANEOUS BUCKLING MODES

When a stiffened panel made of a given amount of material per unit width is designed so that the critical bifurcation load is the highest possible, Euler-type buckling and local buckling will usually occur simultaneously at the critical load. This can be explained by the following argument: when the plate thickness is increased by taking material from the stiffeners and adding it to the plate, the critical load for local buckling is increased and the

critical load for Euler-type buckling is decreased, at most practical combinations of parameters. Thus, the panel with the highest critical bifurcation load usually has simultaneous buckling modes.

The Euler-type buckling mode is denoted $w_c^{(1)}$, $F_c^{(1)}$ and the local buckling mode is denoted $w_c^{(2)}$, $F_c^{(2)}$. Both modes are normalized so that the maximum normal deflection is equal to the plate thickness (i.e. $c_1 + c_2 = h$).

As an example, we carry out a quantitative analysis for a panel defined by the following parameters: $a/b = 4$, $e/b = 5 \cdot 10^{-2}$, $E_s/E = 1$, $A_s/b^2 = 4 \cdot 10^{-3}$, $I_s/b^4 = \frac{1}{3} \cdot 10^{-5}$, $K_s/b^4 = 16 \cdot 10^{-7}$ and $\nu = 0{\cdot}3$. This panel has two simultaneous buckling modes when $h/b = 0{\cdot}8800 \cdot 10^{-2}$ and the corresponding critical value of the load parameter is $\lambda_c = 97{\cdot}44Eh^3/(-N_x^0 a^2)$. Thus, for the panel under consideration, the ratio between the amount of material in the plate and that in the stiffeners is $hb/A_s = 2{\cdot}2$ and the ratio between the area moment of inertia of the cross-section of the plate and that of the stiffeners is $\frac{1}{12}bh^3/I_s = 0{\cdot}017$.

As the solutions are periodic in the y-direction, we need only carry out integrations over a section $ABCD$ of the panel (Fig. 1). Integrating over this part of the structure, we easily verify the orthogonality (3.5) between the two buckling modes. In order to find the coefficients of the algebraic equations (3.10), we evaluate the following integrals

$$-\lambda_c\{\sigma_0, L_2(u_c^{(1)})\} = -\lambda_c\left\{2\int_0^a\int_0^{b/2} N_x^0(w_{c,x}^{(1)})^2\,dy\,dx + \int_0^a N_s^0[(w_{c,x}^{(1)})^2]_{y=b/2}\,dx\right\} \tag{4.1}$$

$$-\lambda_c\{\sigma_0, L_2(u_c^{(2)})\} = -\lambda_c\left\{2\int_0^a\int_0^{b/2} N_x^0(w_{c,x}^{(2)})^2\,dy\,dx + \int_0^a N_s^0[e^2(w_{c,xy}^{(2)})^2]_{y=b/2}\,dx\right\} \tag{4.2}$$

$$\begin{aligned}\{\sigma_c^{(1)}, L_2(u_c^{(1)})\} = 2\int_0^a\int_0^{b/2} &(F_{c,yy}^{(1)}(w_{c,x}^{(1)})^2 - 2F_{c,xy}^{(1)}w_{c,x}^{(1)}w_{c,y}^{(1)} \\ &+ F_{c,xx}^{(1)}(w_{c,y}^{(1)})^2)\,dy\,dx + \int_0^a\left[E_sA_s\left\{\frac{1}{Eh}(F_{c,yy}^{(1)} - \nu F_{c,xx}^{(1)}) \right.\right. \\ &\left.\left. - ew_{c,xx}^{(1)}\right\}(w_{c,x}^{(1)})^2\right]_{y=b/2} dx\end{aligned} \tag{4.3}$$

$$\begin{aligned}\{\sigma_c^{(1)}, L_2(u_c^{(2)})\} = 2\int_0^a\int_0^{b/2} &(F_{c,yy}^{(1)}(w_{c,x}^{(2)})^2 - 2F_{c,xy}^{(1)}w_{c,x}^{(2)}w_{c,y}^{(2)} + F_{c,xx}^{(1)}(w_{c,y}^{(2)})^2)\,dy\,dx \\ &+ \int_0^a\left[E_sA_s\left\{\frac{1}{Eh}(F_{c,yy}^{(1)} - \nu F_{c,xx}^{(1)}) - ew_{c,xx}^{(1)}\right\}e^2(w_{c,xy}^{(2)})^2\right]_{y=b/2} dx\end{aligned} \tag{4.4}$$

$$\{\sigma_c^{(1)}, L_{11}(u_c^{(1)}, u_c^{(2)})\} = \{\sigma_c^{(2)}, L_2(u_c^{(1)})\} = \{\sigma_c^{(2)}, L_2(u_c^{(2)})\} = \{\sigma_c^{(2)}, L_{11}(u_c^{(1)}, u_c^{(2)})\} = 0. \tag{4.5}$$

Inserting the expressions (2.13) and (2.14) for the buckling modes in equations (4.1)–(4.4) and carrying out the integrations, we find that the equilibrium relations (3.10) between λ, ξ_1 and ξ_2 are

$$\left(1 - \frac{\lambda}{\lambda_c}\right)\xi_1 + d_1\xi_1^2 + d_2\xi_2^2 = \frac{\lambda}{\lambda_c}\bar{\xi}_1 \tag{4.6}$$

$$\left(1 - \frac{\lambda}{\lambda_c}\right)\xi_2 + d_3\xi_1\xi_2 = \frac{\lambda}{\lambda_c}\bar{\xi}_2 \tag{4.7}$$

where the non-dimensional coefficients are

$$d_1 = \tfrac{3}{2}\{\sigma_c^{(1)}, L_2(u_c^{(1)})\}/\{-\lambda_c\sigma_0, L_2(u_c^{(1)})\} = -0{\cdot}0193 \tag{4.8}$$

$$d_2 = \tfrac{1}{2}\{\sigma_c^{(1)}, L_2(u_c^{(2)})\}/\{-\lambda_c\sigma_0, L_2(u_c^{(1)})\} = -0{\cdot}6731 \tag{4.9}$$

$$d_3 = \{\sigma_c^{(1)}, L_2(u_c^{(2)})\}/\{-\lambda_c\sigma_0, L_2(u_c^{(2)})\} = -0{\cdot}1138. \tag{4.10}$$

For the perfect panel ($\bar{\xi}_1 = \bar{\xi}_2 = 0$), the post-buckling variation of ξ_1 and ξ_2 with λ is found by solving equations (4.6) and (4.7) with respect to ξ_1 and ξ_2

$$\xi_1 = -\frac{1}{d_3}\left(1-\frac{\lambda}{\lambda_c}\right) \tag{4.11}$$

$$\xi_2 = \pm\sqrt{\left(\frac{d_3-d_1}{d_2 d_3^2}\right)\left(1-\frac{\lambda}{\lambda_c}\right)}. \tag{4.12}$$

These post-buckling branches are shown in Fig. 2, and we recall that ξ_1 or ξ_2 equal to unity means a maximum deflection equal to the plate thickness.

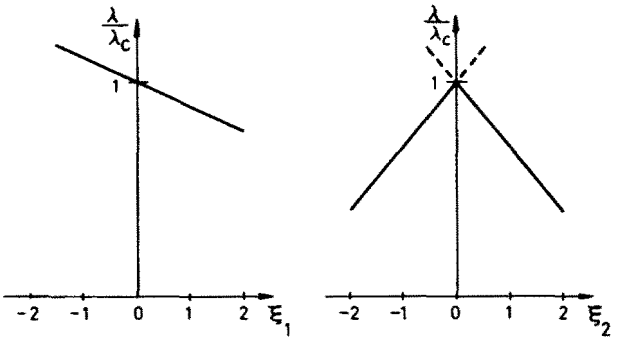

FIG. 2. Dependence on load of mode deflections.

For the perfect panel, the generalized displacement in equation (3.11) corresponds to the average reduction of distance between the edges of the panel. Substituting equations (4.11) and (4.12) in equation (3.11) and evaluating the integrals, we find the following load–compression relation for the panel in consideration

$$\frac{\Delta}{\lambda_c\Delta_0} = \frac{\lambda}{\lambda_c} + 4{\cdot}5687\,.\left(1-\frac{\lambda}{\lambda_c}\right)^2. \tag{4.13}$$

The initial part of this curve is shown in Fig. 3.

When imperfections are present only in the shape of the Euler buckling mode ($\bar{\xi}_1 > 0$, $\bar{\xi}_2 = 0$), ξ_1 grows with increasing λ according to

$$\xi_1 = \frac{1}{2d_1}\left[\sqrt{\left\{\left(1-\frac{\lambda}{\lambda_c}\right)^2 + 4d_1\bar{\xi}_1\frac{\lambda}{\lambda_c}\right\}} - \left(1-\frac{\lambda}{\lambda_c}\right)\right] \tag{4.14}$$

while the parameter ξ_2 remains equal to zero until the coefficient of ξ_2 in equation (4.7) disappears. At this point, bifurcation in the shape of the local buckling mode occurs and

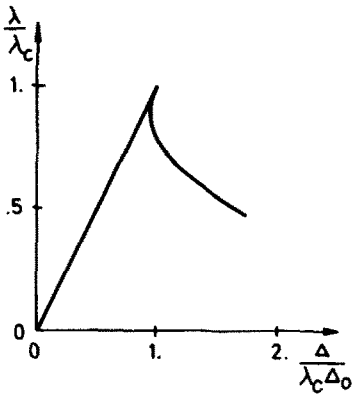

FIG. 3. Relationship between load and compression for a perfect panel.

the equilibrium load falls, with deflections occurring in both modes. The maximum value λ^* of the load parameter can be found from the equation

$$\left(1-\frac{\lambda^*}{\lambda_c}\right)^2+\frac{d_3^2}{d_3-d_1}\bar{\xi}_1\frac{\lambda^*}{\lambda_c}=0. \tag{4.15}$$

When there are also imperfections in the shape of the local buckling mode ($\bar{\xi}_2 \neq 0$), we find, by eliminating ξ_1 from equations (4.6) and (4.7), the following relation between λ and ξ_2

$$\begin{aligned}\left(\frac{\lambda}{\lambda_c}\right)^2&\left\{\xi_2^2\left(1-\frac{d_3}{d_1}\right)+2\xi_2\bar{\xi}_2\left(1-\frac{d_3}{2d_1}\right)+\bar{\xi}_2^2\right\}\\&+\frac{\lambda}{\lambda_c}\left\{2\xi_2^2\left(\frac{d_3}{d_1}-1-\frac{d_3^2}{2d_1}\bar{\xi}_1\right)-2\xi_2\bar{\xi}_2\left(1-\frac{d_3}{2d_1}\right)\right\}\\&+\left\{\xi_2^2\left(1-\frac{d_3}{d_1}\right)+\xi_2^4\frac{d_3^2d_2}{d_1}\right\}=0.\end{aligned} \tag{4.16}$$

This equation and the condition $d\lambda/d\xi_2 = 0$ give an expression analogous to (4.15) for the maximum load parameter λ^*. However, as this expression becomes considerably more complicated than (4.15), we have preferred to determine λ^* from a plot of λ against ξ_2. The results shown in Fig. 4 indicate that the panel is more sensitive to imperfections in the shape of the local buckling mode than to imperfections in the shape of the Euler buckling mode.

All the preceding calculations have been made for one particular geometry of the panel. Now the influence of the eccentricity of the stringers can be illustrated by calculating the slopes of the branches at the bifurcation point (analogous to those shown in Fig. 2) as a function of the parameter e/b, still choosing the plate thickness so that the two buckling modes coincide and keeping all other parameters unchanged. The curves in Fig. 5 show that for values of e/b equal to about $\frac{1}{4}$ and equal to zero, a higher order analysis would be necessary to investigate imperfection-sensitivity. However, the interval $0 < |e/b| < \frac{1}{4}$ is representative of a large range of practical structures, where the behaviour is qualitatively as illustrated by the example chosen above. From Fig. 5 we see that the number of half

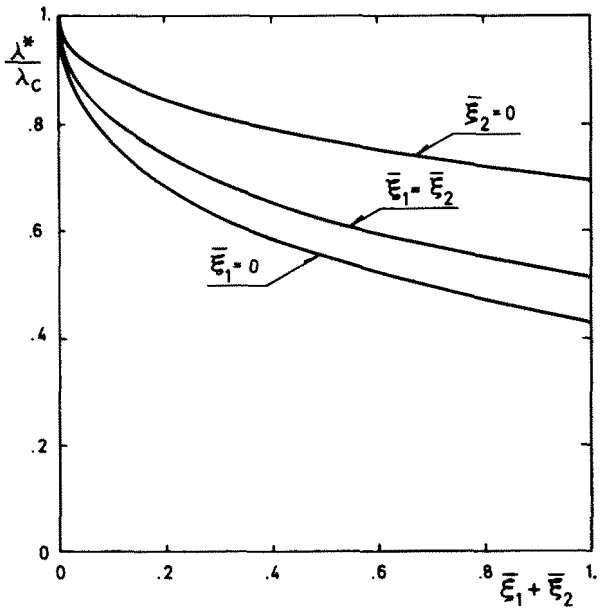

FIG. 4. Carrying capacity of imperfect panel.

waves of the local buckling mode corresponding to the smallest critical load changes at two values of e/b. In these special cases there are three operative buckling modes. However, this will not be further discussed here as the behaviour in this three-mode case is not expected to differ significantly from the behaviour in the two-mode case just discussed.

5. A SINGLE BUCKLING MODE

In this section we shall determine the initial post-buckling behaviour of a panel with only a single critical buckling mode. For given values of all other parameters than the plate

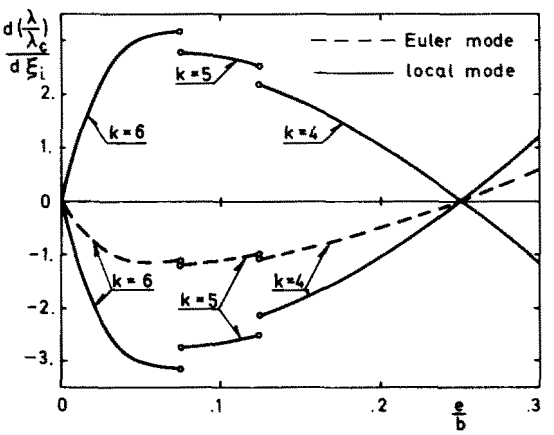

FIG. 5. Slopes of the equilibrium branches at the bifurcation point for different values of the eccentricities of the stiffeners. The special case $e/b = 0{\cdot}05$ is identical to the case shown in Fig. 2.

thickness, the two-mode case discussed in Section 4 takes place at one particular value h_0 of the plate thickness. For thicknesses smaller than h_0, local buckling occurs first, while for greater thicknesses, Euler-type buckling occurs first.

In order to find the coefficient b in the asymptotic expansion (3.6), we must calculate a higher order contribution to the displacement field after bifurcation. In the vicinity of the bifurcation point we write the solution of our problem as the expansion

$$\begin{pmatrix} w \\ F \end{pmatrix} = \lambda \begin{pmatrix} 0 \\ F_0 \end{pmatrix} + \xi \begin{pmatrix} w_c \\ F_c \end{pmatrix} + \xi^2 \begin{pmatrix} w_2 \\ F_2 \end{pmatrix} + \dots . \tag{5.1}$$

Substituting this expansion in the nonlinear equations (1.9) and (1.10), we find the following equations for the second order contributions w_2 and F_2

$$D\,\Delta\Delta w_2 - \lambda_c N_x^0 w_{2,xx} = a\lambda_c N_x^0 w_{c,xx} + F_{c,yy} w_{c,xx} - 2F_{c,xy} w_{c,xy} + F_{c,xx} w_{c,yy} \tag{5.2}$$

$$\frac{1}{Eh}\Delta\Delta F_2 = w_{c,xy}^2 - w_{c,xx} w_{c,yy}. \tag{5.3}$$

The linear boundary conditions are derived in the same way from equations (1.11)–(1.21), but we shall omit the expressions here. We must further require that no more than the prescribed load λN_s^0 is applied to the ends of the stiffeners. Consequently, we have to make sure that the force N_{s2}, given by the expression

$$N_{s2} = E_s A_s \left\{ \frac{1}{Eh}(F_{2,yy} - \nu F_{2,xx}) - e w_{2,xx} + \tfrac{1}{2} e^2 w_{c,xy}^2 \right\} \tag{5.4}$$

vanishes at $x = 0, a$. Here the last term on the right-hand side is different from zero in the case of local buckling.

As the right-hand sides in the linear boundary value problem are symmetrical about all planes of type $y = 0$ and $y = b/2$ (Fig. 1), the solutions w_2, F_2 will have the same property. The boundary value problem is solved numerically by taking $w_2(x, y)$ and $F_2(x, y)$ as sine-series in the x-direction and using a finite difference method to determine the y-dependent coefficient functions of the series.

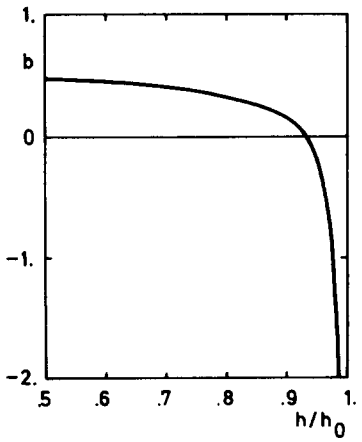

FIG. 6. Post-buckling coefficient b when local buckling occurs first.

In the examples calculated below, the numerical values of all parameters except the plate thickness are chosen equal to the values used in the example in the last section.

When local buckling occurs first, we find that the coefficient a of the asymptotic expansion (3.6) disappears identically, and the coefficient b varies as shown in Fig. 6. When $h/h_0 < 0{\cdot}93$ the panel can carry more axial compression than the load corresponding to local buckling. Above this range the panel becomes still more sensitive to imperfections in the shape of the buckling mode as h/h_0 tends towards unity. The constant K in equation (3.9) gives the relation between the slope of the tangent to the post-buckling curve at the bifurcation point and the slope of the pre-buckling curve. For different values of h/h_0 such tangents are shown in Fig. 7.

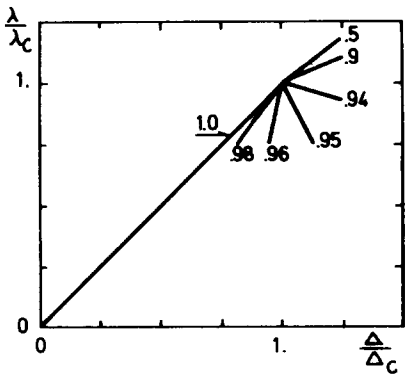

FIG. 7. Tangents to post-buckling curve at bifurcation point for the values of h/h_0 indicated in the diagram.

When Euler-type buckling occurs first, the coefficient a has the values given in Fig. 8. For h/h_0 equal to unity, the value of a is equal to the value of d_1 in equation (4.6). As the values obtained for a only indicate a rather weak sensitivity to imperfections, the second order analysis has also been carried out. This analysis gave the values of b shown in Fig. 8 and thus no significant contribution compared with the first order analysis.

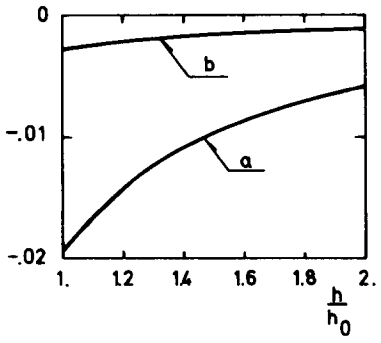

FIG. 8. Post-buckling coefficients a and b when Euler buckling occurs first.

It should be emphasized that for values of h/h_0 close to unity, the single mode initial post-buckling analyses are only adequate in the immediate vicinity of the critical bifurcation point. As discussed by Koiter [13] this is due to the presence of the other buckling mode corresponding to a buckling stress only slightly above the critical stress, with a nonlinear coupling between the two buckling modes.

CONCLUSIONS

The initial post-buckling behaviour of a wide, integrally stiffened panel has been determined. It has been demonstrated that a panel designed so that the critical bifurcation load for the perfect structure attains a given value with a minimum use of material is usually very sensitive to geometrical imperfections. Thus, as imperfections cannot be avoided in practical structures, one has to take into account such irregularities before being able to find a real optimum design.

Acknowledgement—The author wishes to thank Professor John W. Hutchinson, Harvard University, for many valuable comments on the present paper.

REFERENCES

[1] F. CAMPUS and C. MASSONET, Colloque sur le comportement postcritique des plaques utilisées en construction métallique, Interventions de W. T. KOITER et M. SKALOUD, pp. 64–68, 103, 104. Mémoires de la Société Royale des Sciences de Liege, 5me série, tome VIII, fascicule 5 (1963).
[2] A. VAN DER NEUT, The interaction of local buckling and column failure of thin-walled compression members, *Proc. Twelfth Int. Congr. Appl. Mech.*, Stanford University (1968). Springer-Verlag (1969).
[3] W. T. KOITER and G. D. C. KUIKEN, The interaction between local buckling and overall buckling on the behaviour of built-up columns, Delft Laboratory Report WTHD 23 (1971).
[4] J. M. T. THOMPSON and G. M. LEWIS, On the optimum design of thin-walled compression members. *J. Mech. Phys. Solids* **20**, 101–109 (1972).
[5] W. T. KOITER, Buckling and post-buckling behaviour of a cylindrical panel under axial compression, NLR Report S. 476, Nat. Aero. Res. Inst., Vol. 20 Amsterdam (1956).
[6] W. B. STEPHENS, Imperfection sensitivity of axially compressed stringer reinforced cylindrical panels under internal pressure. *AIAA Jnl* **9**, 1713–1719 (1971).
[7] W. T. KOITER, Over de stabiliteit van het elastisch evenwicht, Thesis, Delft, H. J. Paris, Amsterdam (1945); English translation published as NASA TT F-10, 833 (1967).
[8] W. T. KOITER, Elastic stability and post-buckling behaviour. *Proc. Symp. Nonlinear Problems*, pp. 257–275. University of Wisconsin Press (1963).
[9] B. BUDIANSKY and J. W. HUTCHINSON, Dynamic buckling of imperfection-sensitive structures, *Proc. XI Int. Congr. Appl. Mech.*, Munich, pp. 636–651. Springer-Verlag (1964).
[10] B. BUDIANSKY, Dynamic buckling of elastic structures: criteria and estimates, *Proc. Int. Conf. on Dynamic Stability of Structures*, Northwestern University, Evanston. Pergamon Press (1965).
[11] J. W. HUTCHINSON, Imperfection sensitivity of externally pressurized spherical shells. *J. appl. Mech.* **34**, 49–55 (1967).
[12] B. BUDIANSKY, Post-buckling behaviour of cylinders in torsion, *Proc. Second IUTAM Symp. on the Theory of Thin Shells*, Copenhagen, edited by F. I. NIORDSON. Springer (1969).
[13] W. T. KOITER, The nonlinear buckling problem of a complete spherical shell under uniform external pressure. *Proc. Kon. Ned. Ak. Wet.* **B72**, 40–123 (1969).

APPENDIX

Solution of eigenvalue problem

To determine the critical load and the buckling mode, we find by the method outlined in section 2 eight linear, homogeneous equations

$$\sum_{j=1}^{8} g_{ij}c_j = 0, \quad \text{for } i = 1, 2, \ldots, 8.$$

The coefficient matrix has 64 components, 28 of which are equal to zero. The remainder are given by the following expressions, where according to equation (2.15), r_1 and r_2 depend on λ_c

$$g_{13} = -g_{17} = \cosh\frac{k\pi b}{2a}$$

$$g_{14} = -g_{18} = \frac{b}{2}\sinh\frac{k\pi b}{2a}$$

$$g_{21} = E_sA_se\left(\frac{k\pi}{a}\right)^2\cosh\frac{r_1 b}{2}$$

$$g_{22} = E_sA_se\left(\frac{k\pi}{a}\right)^2\cos\frac{r_2 b}{2}$$

$$g_{23} = \frac{k\pi}{a}\sinh\frac{k\pi b}{2a} + \frac{E_sA_s}{Eh}\left(\frac{k\pi}{a}\right)^2\cosh\frac{k\pi b}{2a}(1+\nu)$$

$$g_{24} = \sinh\frac{k\pi b}{2a}\left\{1+\frac{E_sA_sb}{2Eh}\left(\frac{k\pi}{a}\right)^2(1+\nu)\right\} + \frac{k\pi b}{2a}\cosh\frac{k\pi b}{2a}\left(1+4\frac{E_sA_s}{Ehb}\right)$$

$$g_{27} = \frac{k\pi}{a}\sinh\frac{k\pi b}{2a}$$

$$g_{28} = \sinh\frac{k\pi b}{2a} + \frac{k\pi b}{2a}\cosh\frac{k\pi b}{2a}$$

$$g_{31} = Dr_1^3\sinh\frac{r_1 b}{2} - \left(\frac{k\pi}{a}\right)^2\left\{E_sI_s\left(\frac{k\pi}{a}\right)^2 + \lambda_c N_s^0\right\}\cosh\frac{r_1 b}{2}$$

$$g_{32} = Dr_2^3\sin\frac{r_2 b}{2} - \left(\frac{k\pi}{a}\right)^2\left\{E_sI_s\left(\frac{k\pi}{a}\right)^2 + \lambda_c N_s^0\right\}\cos\frac{r_2 b}{2}$$

$$g_{33} = g_{37} = e\left(\frac{k\pi}{a}\right)^3\sinh\frac{k\pi b}{2a}$$

$$g_{34} = g_{38} = e\left(\frac{k\pi}{a}\right)^2\left(\sinh\frac{k\pi b}{2a} + \frac{k\pi b}{2a}\cosh\frac{k\pi b}{2a}\right)$$

$$g_{35} = Dr_1^3\sinh\frac{r_1 b}{2}$$

$$g_{36} = Dr_2^3 \sin\frac{r_2 b}{2}$$

$$g_{41} = -Dr_1^2 \cosh\frac{r_1 b}{2} - \left(\frac{k\pi}{a}\right)^2 (G_s K_s + e^2 \lambda_c N_s^0) r_1 \sinh\frac{r_1 b}{2}$$

$$g_{42} = Dr_2^2 \cos\frac{r_2 b}{2} + \left(\frac{k\pi}{a}\right)^2 (G_s K_s + e^2 \lambda_c N_s^0) r_2 \sin\frac{r_2 b}{2}$$

$$g_{45} = Dr_1^2 \cosh\frac{r_1 b}{2}$$

$$g_{46} = -Dr_2^2 \cos\frac{r_2 b}{2}$$

$$g_{53} = -g_{57} = -\left(\frac{k\pi}{a}\right)^2 \cosh\frac{k\pi b}{2a}$$

$$g_{54} = -g_{58} = -\frac{2k\pi}{a}\cosh\frac{k\pi b}{2a} - \frac{b}{2}\left(\frac{k\pi}{a}\right)^2 \sinh\frac{k\pi b}{2a}$$

$$g_{63} = g_{67} = \left(\frac{k\pi}{a}\right)^3 \sinh\frac{k\pi b}{2a}(1+\nu)$$

$$g_{64} = g_{68} = -\left(\frac{k\pi}{a}\right)^2 \sinh\frac{k\pi b}{2a}(1-\nu) + \frac{b}{2}\left(\frac{k\pi}{a}\right)^3 \cosh\frac{k\pi b}{2a}(1+\nu)$$

$$g_{71} = -g_{75} = -\cosh\frac{r_1 b}{2}$$

$$g_{72} = -g_{76} = -\cos\frac{r_2 b}{2}$$

$$g_{81} = g_{85} = -r_1 \sinh\frac{r_1 b}{2}$$

$$g_{82} = g_{86} = r_2 \sin\frac{r_2 b}{2}.$$

By equating the determinant of the coefficient matrix to zero, we find a rather complicated transcendental equation for the critical load parameter λ_c. The equation is solved numerically by a systematic search for the lowest zero point.

(*Received* 24 *January* 1972; *revised* 20 *March* 1972)

Абстракт—Определяется начальное поведение в закритической области для полностью усиленной, широкой панели, под влиянием сжимаемой нагрузки. Исследуются полное выпучивание панели, в смисле широкой колонны Эйлера, и также местное выпучивание пластинок между ребрами жесткости.

Расчет панели приводится для следующих предположений: критическая нагрузка бифуркации найбольша из всех возможных для заданного количества материала на единицу ширины, что приводит к конструкции, в которой потера устойчивости по Эйлеру и местное выпучивание происходят одновременно. Указывается, что такая панель очень чувствительна к геометрическим неточностям. Затем, критическая нагрузка бифуркации не может быть достижена для практической конструкции. Исследование двух форм расчета не всегда оказывается расчетом на оптимум материала.